Copyright Warning & Restrictions

The copyright law of the United States (Title 17, United States Code) governs the making of photocopies or other reproductions of copyrighted material.

Under certain conditions specified in the law, libraries and archives are authorized to furnish a photocopy or other reproduction. One of these specified conditions is that the photocopy or reproduction is not to be "used for any purpose other than private study, scholarship, or research." If a, user makes a request for, or later uses, a photocopy or reproduction for purposes in excess of "fair use" that user may be liable for copyright infringement,

This institution reserves the right to refuse to accept a copying order if, in its judgment, fulfillment of the order would involve violation of copyright law.

Please Note: The author retains the copyright while the New Jersey Institute of Technology reserves the right to distribute this thesis or dissertation

Printing note: If you do not wish to print this page, then select "Pages from: first page # to: last page #" on the print dialog screen

ABSTRACT

ORTHOGONAL SPACE TIME CODING FOR IM/DD OPTICAL WIRELESS COMMUNICATION WITH SINGLE CARRIER FREQUENCY DOMAIN EQUALIZATION

by
Nan Wu

Recently the development of optical wireless communication has received growing attention because of its unlimited bandwidth and simple implementation as compared to radio frequency communication application for indoor wireless data transmission. The objective of this thesis is to improve the performance of intensity-modulated direct-detection (IM/DD) optical wireless communications with single carrier frequency domain equalization (SCFDE) by using Orthogonal Space Time Code (OSTC). More attention has been paid to three SCFDE schemes due to their outstanding performances in practical cases. It is demonstrated that OSTC can be modified to be suitable to optical systems and provide an excellent enhancement to system performances. By applying 4×4 OSTC that was formally used extensively in radio frequency communications, the performance of optical wireless systems with SCFDE is to be improved remarkably. It is pointed out that there exist some differences of the application of OSTC in between radio frequency communications and optical wireless communications. The performances, such as Peak-to-average Power ratio, complexity and Bit-error rate, are compared and discussed. Finally the optical system, which has the best performance, is proposed and extended with multiple LEDs and Photodiodes.

ORTHOGONAL SPACE TIME CODING FOR IM/DD OPTICAL WIRELESS COMMUNICATION WITH SINGLE CARRIER FREQUENCY DOMAIN EQUALIZATION

by
Nan Wu

A Thesis
Submitted to the Faculty of
New Jersey Institute of Technology
in Partial Fulfillment of the Requirements for the Degree of
Master of Science in Electrical Engineering

Department of Electrical and Computer Engineering

August 2011

APPROVAL PAGE

ORTHOGONAL SPACE TIME CODING FOR IM/DD OPTICAL WIRELESS COMMUNICATION WITH SINGLE CARRIER FREQUENCY DOMAIN EQUALIZATION

Nan Wu

Dr. Yeheskel Bar-Ness, Thesis Advisor — Date
Distinguished Professor of Electrical and Computer Engineering, NJIT

Dr. Ali Abdi, Committee Member — Date
Associate Professor of Electrical and Computer Engineering, NJIT

Dr. Osvaldo Simeone, Committee Member — Date
Assistant Professor of Electrical and Computer Engineering, NJIT

BIOGRAPHICAL SKETCH

Author: Nan Wu

Degree: Master of Science

Date: August 2011

Undergraduate and Graduate Education:

- Master of Science in Electrical Engineering,
  New Jersey Institute of Technology, Newark, NJ, 2011

- Bachelor of Science in Communication Engineering,
  Anhui Normal University, Wuhu, Anhui, 2009

Major: Electrical Engineering

Presentations and Publications:

Y. Bar-Ness, N. Wu, "Space Time Coding for IM/DD Optical Wireless Communication using DQO-SCFDE," Submitted to IEEE Globecom 2011.

ACKNOWLEDGMENT

First and foremost, I would like to show my deepest gratitude to my supervisor, Dr. Yeheskel Bar-Ness, a respectable and responsible scholar, who has provided me with valuable guidance during my graduate study. Without his enlightening instruction, kindness and patience, I could not have completed my thesis.

I shall extend my thanks to all my professors at New Jersey Institute of Technology, especially Dr. Durga Misra for the great help for my graduate study and life. My sincere appreciation also goes to all of my friends. In particular, I would like to thank: my MS thesis committee members: Yeheskel Bar-Ness, Ali Abdi and Osvaldo Simeone; my colleagues from the Center for Wireless Communication & Signal Processing Research: Kodzovi Acolatse, Amir Laufer, Xiaoli Wang, Chen Chen, Yuewen Wang and Yu Liu. Finally, but not the least, my family and my girlfriend.

TABLE OF CONTENTS

TABLE OF CONTENTS
(Continued)

LIST OF TABLES

LIST OF FIGURES

CHAPTER 1

INTRODUCTION

1.1 Objective

The objective of this thesis is to improve the performance of intensity-modulated direct-detection (IM/DD) optical wireless communications with single carrier frequency domain equalization (SCFDE) by using Orthogonal Space Time Code (OSTC).

Thus far several optical wireless communication systems with SCFDE have been proposed. Among these, more attention has been paid to three SCFDE schemes due to the outstanding performance in practical cases. They are the Asymmetrically Clipped Optical Single Carrier Frequency domain Equalization (ACO-SCFDE), the Repetition and Clipping Optical Single Carrier Frequency domain Equalization (RCO-SCFDE) and the Decomposed Quadrature Optical Single Carrier Frequency Domain Equalization (DQO-SCFDE). They used only one LED emitter deployed at transmitter and one photodiode at receiver. By applying 4×4 OSTC to these three schemes, four LED emitters are deployed to transmit four independent optical data streams at the same time. The performances, such as Peak-to-average Power ratio, complexity and Bit-error rate, will be compared and discussed in the following several chapters. The scheme, which has the most advantages, will be proposed and finally be extended to four LED emitters and two photodiodes by using Multi Input Multi Output technique. By applying these wireless techniques that were formally used extensively in radio frequency communications, the performance of optical wireless systems with SCFDE is to be improved remarkably.

1.2 Introduction of Optical Wireless Communications

Communications are crucial for old and modern societies. In all the aspects of society, in order to deal with different things appropriately, people usually make right decisions after they get the right information by different communications schemes. Moreover, optical communication was already used long time ago. In ancient China, soldiers lit fire on the Great Wall to transmit military information as whether the enemy invaded the border or not. In modern society, light communication is used extensively in various aspects. Landing lights are used in aircraft to land safely, especially during the night. Traffic lights indicate when to cross or when to stop.

Obviously, light communications are the simplest form of optical communications. It is a form of telecommunication that uses light, which is invisible, to transmit information in optical channels. There are two branches of optical communications; the optical fiber communication (OFC) and the optical wireless communications (OWC). The former is the most common approaches for modern digital optical communication. However, recently OWC has been used in various applications. Compared with OFC, OWC can be employed much easier because it does not require deploying fiber underground. Another wireless communication technique, radio frequency communication, which has only limited spectrum, will be no longer sufficient to satisfy the demand of high speed data transmission as the increasing number of portable information terminals. Therefore the development of optical wireless communication received growing attention because of its unlimited bandwidth and simple implementation as compared to radio frequency communication application for indoor wireless data transmission [1]. Optical wireless communication can be an effective

alternative to radio frequency communication particularly for indoor use. In OW system, light emitting diodes (LED) and photodiodes are used as transmitter and receiver respectively. The Block diagram of intensity-modulated direct-detection (IM/DD) optical wireless systems is shown in Figure 1.1.

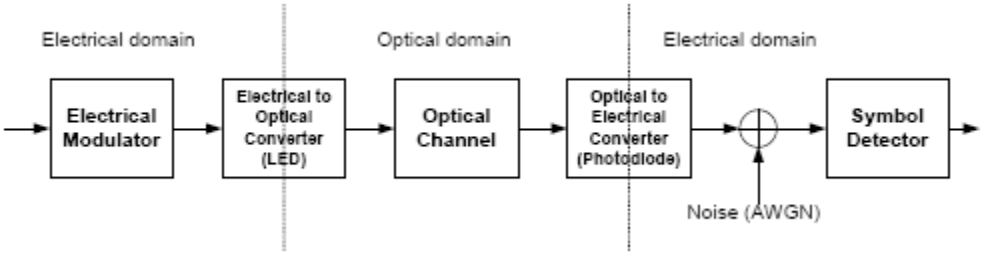

Figure 1.1 Block diagram of IM/DD optical wireless systems. [10]

1.3 Wireless Communications Techniques

1.3.1 OFDM and SCFDE

Orthogonal Frequency Division Multiplexing (OFDM) [2] is a multi-carrier digital modulation technique in which a high bit rate serial data streams is divided into a large number N of low data rate streams, one modulating each sub-carrier. Each sub-carrier is modulated with conventional modulation scheme, such as QPSK, 16-QAM and 64-QAM, depending on how severe the channel condition is. The better the channel condition is the higher constellation used. In OFDM, the sub-carrier frequencies are chosen such that their spectra are orthogonal to each other and the cross-talk between sub-channels, which is called inter-carrier interference (ICI), is eliminated even if the spectra are overlapped in frequency domain and inter-carrier guard bands are not required. However in order to avoid inter-symbol interference (ISI) caused by multi-path propagation delay in a

frequency-selective fading environment, a guard intervals in a form cyclic prefix (CP) are introduced between consecutive blocks of data symbols. Due to these facts, OFDM can cope with sever channel conditions without complex equalizer. Because data modulate different frequencies, the amplitude of transmitted signal will fluctuate intensively. This is an inherent main drawback of OFDM, termed high **Peak-to-Average Power Ratio (PAPR)**. The transceiver block diagram of OFDM is shown in Figure 1.2.

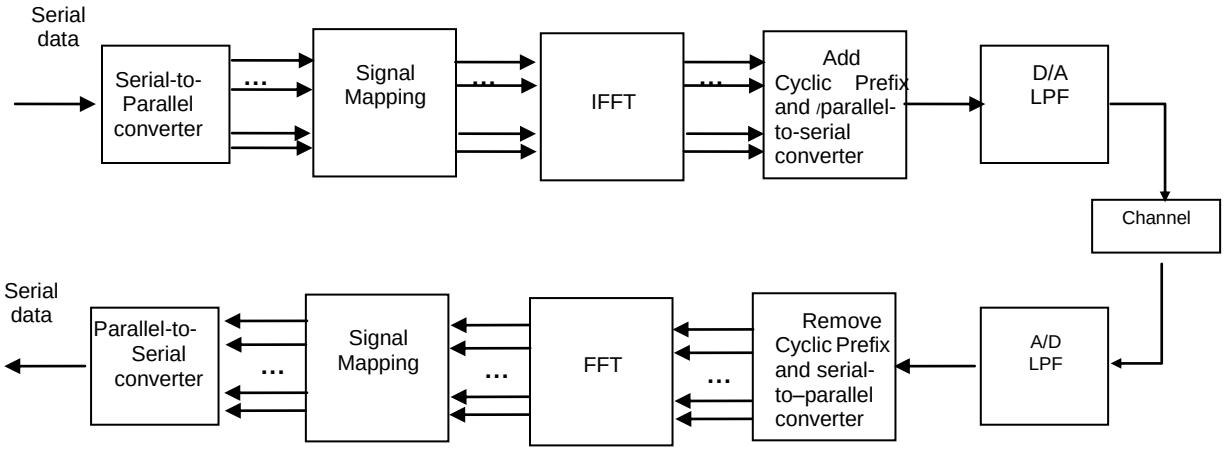

Figure 1.2 Block diagram of OFDM.

Single Carrier Frequency Domain Equalization (SCFDE) [3] is a blocked single carrier transmission scheme with frequency domain equalization at receiver. This scheme has a reduced complexity at the transmitter because it does not require an N-Point FFT block to modulate and divide one data stream to N sub-channels. Due to the fact that the transmitted signal is modulated using single frequency, it can achieve much lower PAPR than that of OFDM. Like OFDM, CP is introduced between consecutive blocks of data symbols to transform the linear convolution of the channel into a circular one. After removing CP at receiver, the received signal will be parsed into frequency domain

equalizers, located between an FFT and an IFFT blocks. It has been proved that frequency domain equalization requires much less computational complexity than conventional time domain equalization. The transceiver block diagram of SCFDE is presented in Figure 1.3.

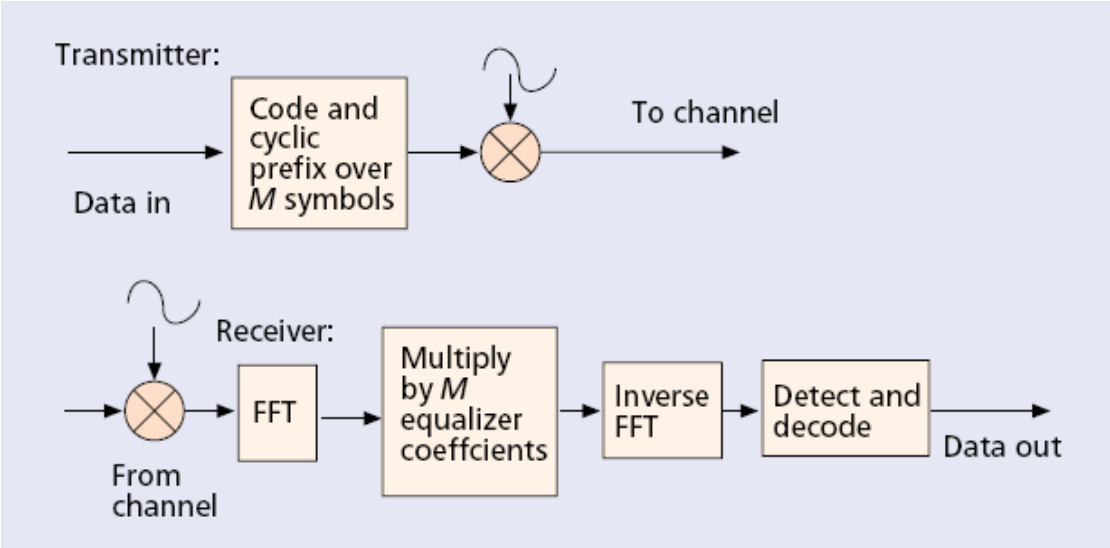

Figure 1.3 Block diagram of SCFDE. [3]

Therefore, Orthogonal Frequency Division Multiplexing (OFDM) and Single Carrier Frequency Domain Equalization (SCFDE) are considered as two effective means for combating inter-symbol-interference (ISI) resulting from multipath propagation. Since OFDM has inherently high Peak-to-Average-Power, which means it requires a wide dynamic power range, the DC-biased optical OFDM (DCO-OFDM) [4] and asymmetrically clipped optical OFDM (ACO-OFDM) [5] are severely affected by the nonlinear response of LED. Hence low PAPR, SCFDE has been considered as an appropriate approach for use in OW system.

1.3.2 MIMO and OSTC

Multiple-Input-Multiple-Output (MIMO) [6] is a well-established smart antenna technique which employs multiple antennas at both transmitter and receiver. It is extensively used to increase the overall capacity of the system and improve data transmission rate. MIMO can be divided into three main categories, beam forming, spatial multiplexing and diversity coding. In beam forming, the same signal is transmitted by each of the multiple antennas such that the transmitted signal is maximized at receiver end. In spatial multiplexing, a high speed data stream is divided into multiple low speed data sub-stream, where each one is transmitted by different antennas at the same frequency. If the antennas are deployed with sufficient spatial distance, the receiver is able to separate different data sub-stream without any aid of frequency or time resource. The channel capacity can be increased remarkably in function of high Signal-to-Noise Ratio. In diversity coding, the same signal is emitted several times using space time coding to increase diversity gain as well as to combat inter-symbol interference. Space time coding (STC) is a promising coding technique used in MIMO, which provides full diversity and low complexity for wireless communications. It makes the transmitted signals orthogonal to each other and explores the independent fading in multiple antennas leading to signal gain enhancement. A number of papers have shown that it provided important benefit in optical systems. However conventional STC cannot be used directly in OW system because it usually requires complex signals and variable polarity for transmission. In this thesis, Orthogonal STC (OSTC) [9] is applied in SCFDE optical system with suitable modification. It is demonstrated not only that OSTC is feasible in ACO-SCFDE, RCO-SCFDE and DQO-SCFDE, but it also achieves excellent

performance when applied to optical wireless communications.

CHAPTER 2

ASYMMETRICALLY CLIPPED OPTICAL SINGLE CARRIER FREQUENCY DOMAIN EQUALIZATION (ACO-SCFDE) WITH ORTHOGONAL SPACE TIME CODE

In this chapter, asymmetrically clipped method is applied to SCFDE to obtain ACO-SCFDE with low PAPR. Due to the fact that only real and positive signal can be transmitted in optical channel, original SCFDE cannot be directly applied to OWC. Some researchers apply asymmetrically clipped method to OFDM to realize IM/DD OW system. However, since the main disadvantage of OFDM is high PAPR, which largely limits the performance of ACO-OFDM, ACO-SCFDE will be paid much more attention rather than ACO-OFDM. Therefore the ACO-SCFDE scheme will be presented in detail. Therefore, OSTC will be applied in ACO-SCFDE and a comparison between these two ACO-SCFDEs will be given in Chapter 5.

2.1 Review of Asymmetrically Clipped Optical Single Carrier Frequency Domain Equalization (ACO-SCFDE)

Block diagram of ACO-SCFDE is shown in Figure 2.1(a). First, one block of N complex data symbols $\mathbf{s} = [s_0, s_1, \dots \dots s_{N-1}]$ drawn from QPSK constellation is inputted to an N-point FFT to produce the frequency domain vector; $\mathbf{S} = [S_0, S_1, \dots \dots S_{N-1}]$. Then, in order to obtain the Hermitian constraint, N symbols of S are mapped to 2N Hermitian symmetric symbols and zeros are added to form a 4N×1 vector; $\mathbf{X} = [0, S_0, 0, S_1, \dots \dots, 0, S_{N-1}, 0, S_{N-1}^*, 0, S_{N-2}^*, \dots \dots , \ 0, S_0^*]$. Next a 4N-point IFFT is

taken to transform the symbols of vector X to time domain; $\mathbf{x} = [x_0, x_1, \ldots\ldots, x_{4N-1}]$. Then to this vector signal a CP will be added to avoid inter-carrier interference as well as inter-block interference. To make the transmitted signal positive, all the negative values are clipped to zero to form the signal vector of $\tilde{\mathbf{x}} = [\tilde{x}_{4N-L}, \ldots\ldots, \tilde{x}_{4N-1}, \tilde{x}_0, \tilde{x}_1, \ldots\ldots, \tilde{x}_{4N-1}]$ whose components are:

$$\tilde{x}_n = \begin{cases} x_n, \text{ if } x_n > 0, \\ 0, \text{ if } x_n <= 0, \end{cases} \tag{2.1}$$

where L is the length of the CP. The ACO-SCFDE symbol structure is shown in Figure 1(b). The time domain signal $\tilde{\mathbf{x}}$ is transmitted through wireless channel **h,** where $\mathbf{h} = [h_0, h_1, \ldots\ldots h_{L-1}]$ is the L-path impulse response of the optical channel. The CP turns the linear convolution with the channel into a circular one:

$$\mathbf{y} = \mathbf{x} \odot \mathbf{h} + \boldsymbol{w}, \tag{2.2}$$

where, **w** is the noise vector without CP. At the receiver, **y** is transformed by a 4N-point FFT block to become, $\mathbf{Y} = \boldsymbol{\Lambda}\mathbf{X} + \mathbf{W}$, where **Y** is frequency domain symbols of **y**, Λ is a 4N×4N matrix whose diagonal elements are the 4N-point FFT of **h** and **W** is the 4N-point FFT of **w**. The odd subcarriers are extracted from **Y** to yield $\mathbf{Y_0} = \boldsymbol{\Lambda_0}\bar{\mathbf{S}} + \mathbf{W_0}$, where $\bar{\mathbf{S}} = \frac{1}{2}[S_0, S_1, \ldots\ldots, S_{N-1}, S^*_{N-1}, S^*_{N-2}, \ldots\ldots, S^*_0]$, where, $\mathbf{Y_0}$ and $\mathbf{W_0}$ are the vectors composed of the odd elements of **Y** and **W**, respectively. To mitigate the effects

of the channel, a minimum mean square error or zero-forcing can be operated on $\mathbf{Y_0}$ to obtain an estimate for $\bar{\mathbf{S}}$; $\hat{\bar{\mathbf{S}}}$ as follows:

$$\hat{\bar{\mathbf{S}}} = (\mathbf{\Lambda_0^H \Lambda_0} + (\mathrm{a/SNR})\mathrm{I_{2N}})^{-1}\Lambda_0^{\mathrm{H}}\mathbf{Y_0} \tag{2.3}$$

where a=1 for MMSE and a=0 for ZF receivers. Due to the Hermitian symmetry condition, the symbols of **S** are repeated in $\bar{\mathbf{S}}$, hence we can add them after conjugation of the second half as follow:

$$\hat{\mathbf{S}} = [\hat{\bar{\mathrm{S}}}]_{\mathrm{k=0}}^{\mathrm{N-1}} + [\hat{\bar{\mathrm{S}}}^{*}(2\mathrm{N} - 1 - \mathrm{k})]_{\mathrm{k=0}}^{\mathrm{N-1}} \tag{2.4}$$

Finally, we use an N-point IFFT to transform $\hat{\mathbf{S}}$ back into time domain to yield the time domain $\hat{\mathbf{s}}$. Hard limiter is then made on the symbol of $\hat{\mathbf{s}}$.

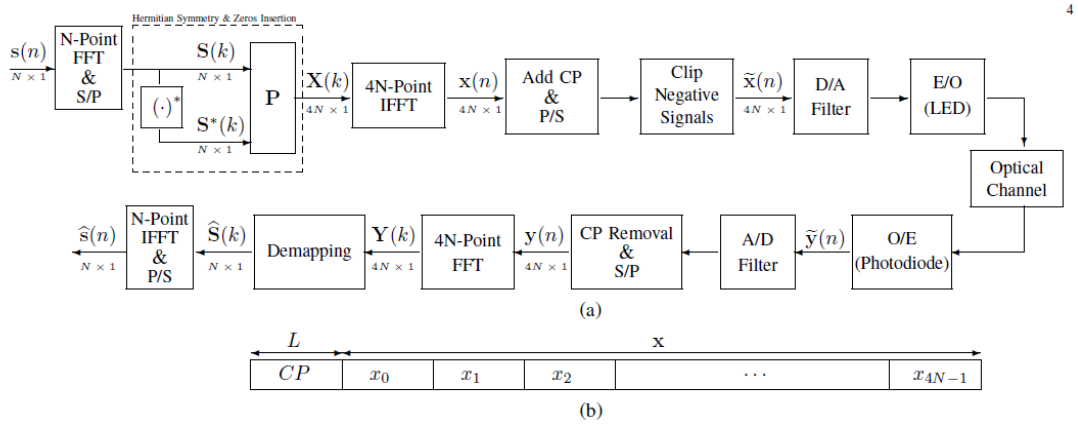

Figure 2.1 (a) ACO-SCFDE Transmitter and Receiver configuration.
(b) ACO-SCFDE symbol after cyclic extension. [10]

2.2 ACO-SCFDE with OSTC

In this section, we apply OSTC in IM/DD optical wireless to ACO-SCFDE. We assume four LEDs employed in the transmitter and one photodiode in the receiver. A **real orthogonal space time code** of size n×n orthogonal matrix with entries values, $\pm x_1, \pm x_2, \ldots, \pm x_n$ are used. For n=4, the 4×4 OSTC is shown below:

$$\mathbf{X_{4*4}} = \begin{bmatrix} x_1 & x_2 & x_3 & x_4 \\ -x_2 & x_1 & -x_4 & x_3 \\ -x_3 & x_4 & x_1 & -x_2 \\ -x_4 & -x_3 & x_2 & x_1 \end{bmatrix} \tag{2.5}$$

Due the constraint of real and positive signal in optical channel, we have to make some appropriate modifications in OSTC matrix. The modified OSTC for optical wireless transmission can be presented in the following form:

$$X_{4*4} = \begin{bmatrix} x_1 & x_2 & x_3 & x_4 \\ \bar{x}_2 & x_1 & \bar{x}_4 & x_3 \\ \bar{x}_3 & x_4 & x_1 & \bar{x}_2 \\ \bar{x}_4 & \bar{x}_3 & x_2 & x_1 \end{bmatrix} \tag{2.6}$$

Using this code, the blocks of symbols x_1, x_2 x_3 and x_4 modulate the LED at consecutive sample times n, n+1, n+2 and n+3 as shown in Table 1 bellow , where $\bar{x}_i = A_i - x_i$ and A_i is the peak amplitude of the vector x_i (i=1, 2, 3, 4).

Table 2.1 ACO-SCFDE Space-Time Coding

	LED1	LED2	LED3	LED4
Time n	x_1	x_2	x_3	x_4
Time n+1	$\bar{x}_2$	x_1	$\bar{x}_4$	x_3
Time n+2	$\bar{x}_3$	x_4	x_1	$\bar{x}_2$
Time n+3	$\bar{x}_4$	$\bar{x}_3$	x_2	x_1

For ACO-SCFDE, four blocks of N complex data symbols are transmitted simultaneously. Each of LEDs is transmitting one of these blocked as in the single case described earlier (Figure 2.1). This is repeated at times n, n+1, n+2 and n+3. After passing through the channel h_1, h_2, h_3 and h_4, respectively, the received signal at these times are given by,

$$\begin{aligned} y_n &= x_1 * h_1 + x_2 * h_2 + x_3 * h_3 + x_4 * h_4 + w_n \\ y_{n+1} &= \bar{x}_2 * h_1 + x_1 * h_2 + \bar{x}_4 * h_3 + x_3 * h_4 + w_{n+1} \\ y_{n+2} &= \bar{x}_3 * h_1 + x_4 * h_2 + x_1 * h_3 + \bar{x}_2 * h_4 + w_{n+2} \\ y_{n+3} &= \bar{x}_4 * h_1 + \bar{x}_3 * h_2 + x_2 * h_3 + x_1 * h_4 + w_{n+3} \end{aligned} \quad (2.7)$$

where w_n, w_{n+1}, w_{n+2}, w_{n+3} are the additive white Gaussian noises at times n, n+1, n+2 and n+3, respectively.

After removing the CP, an FFT block is applied to transform the symbols of each sub-block of y_n, y_{n+1}, y_{n+2} and y_{n+3}, to frequency domain to have;

$$
\begin{aligned}
Y_n &= \Lambda_1 X_1 + \Lambda_2 X_2 + \Lambda_3 X_3 + \Lambda_4 X_4 + W_n \\
Y_{n+1} &= \Lambda_1 \overline{X}_2 + \Lambda_2 X_1 + \Lambda_3 \overline{X}_4 + \Lambda_4 X_3 + W_{n+1} \\
Y_{n+2} &= \Lambda_1 \overline{X}_3 + \Lambda_2 X_4 + \Lambda_3 X_1 + \Lambda_4 \overline{X}_2 + W_{n+2} \\
Y_{n+3} &= \Lambda_1 \overline{X}_4 + \Lambda_2 \overline{X}_3 + \Lambda_3 X_2 + \Lambda_4 X_1 + W_{n+3}
\end{aligned} \tag{2.8}
$$

where, Y_n, Y_{n+1}, Y_{n+2}, Y_{n+3} are the FFT of y_n, y_{n+1}, y_{n+2}, y_{n+3}, respectively. Eq. (2.8) can be rewritten in matrix form as

$$
\begin{bmatrix} Y_n \\ \overline{Y}_{n+1} \\ \overline{Y}_{n+2} \\ \overline{Y}_{n+3} \end{bmatrix} = \begin{bmatrix} \Lambda_1 & \Lambda_2 & \Lambda_3 & \Lambda_4 \\ \Lambda_2 & -\Lambda_1 & \Lambda_4 & -\Lambda_3 \\ \Lambda_3 & -\Lambda_4 & -\Lambda_1 & \Lambda_2 \\ \Lambda_4 & \Lambda_3 & -\Lambda_2 & -\Lambda_1 \end{bmatrix} \begin{bmatrix} X_1 \\ X_2 \\ X_3 \\ X_4 \end{bmatrix} + \begin{bmatrix} W_n \\ W_{n+1} \\ W_{n+2} \\ W_{n+3} \end{bmatrix} \tag{2.9}
$$

where $\overline{Y}_{n+1} = Y_{n+1} - A_2\Lambda_1 - A_4\Lambda_3$, $\overline{Y}_{n+2} = Y_{n+2} - A_3\Lambda_1 - A_2\Lambda_4$, $\overline{Y}_{n+3} = Y_{n+3} - A_4\Lambda_1 - A_3\Lambda_2$. Λ_i (i=1, 2, 3 and 4) is the frequency response of the channel between the i th LED and the photodiode. In vector notation (2.9) is written as,

$$
\mathbf{Z}_{ACO} \triangleq \mathbf{\Lambda}_{ACO} S + \mathbf{W}_{ACO} \tag{2.10}
$$

where $\mathbf{\Lambda}_{ACO}$ is a 4N×4N orthogonal matrix and $\mathbf{\Lambda}_{ACO}{}^{H}\mathbf{\Lambda}_{ACO}$ is a matrix shown below:

$$
\mathbf{\Lambda}_{ACO}{}^{H}\mathbf{\Lambda}_{ACO} = H_{ACO}{}^{2}\mathbf{H_O} =
$$

$$
H_{ACO}{}^{2} \cdot \begin{bmatrix} 1 & H_{O1} & H_{O2} & H_{O3} \\ -H_{O1} & 1 & -H_{O3} & H_{O2} \\ H_{O2} & H_{O3} & 1 & H_{O1} \\ -H_{O3} & H_{O2} & -H_{O1} & 1 \end{bmatrix} \tag{2.11}
$$

$H_{ACO}{}^2$ is the overall channel diversity gain. $H_{ACO}{}^2 = |H_1|^2 + |H_2|^2 + |H_3|^2 + |H_4|^2$. $\mathbf{H_O}$ is the channel dependent interference whose parameters are given by:

$$H_{O1} = \frac{2jIm(H_1^* H_2 + H_4^* H_3)}{H_{ACO}{}^2}$$

$$H_{O2} = \frac{2jIm(H_1^* H_3 + H_2^* H_4)}{H_{ACO}{}^2}$$

$$H_{O3} = \frac{2jIm(H_1^* H_4 + H_3^* H_2)}{H_{ACO}{}^2} \quad (2.12)$$

Note that due to modification to positive terms, the off diagonal parameters H_{Oi} are not zero but pure imaginary.

At the receiver, the odd subcarriers are extracted from Y_i to yield $\mathbf{Y_{jo}}=\mathbf{\Lambda_{jo}}\bar{\mathbf{S}}+\mathbf{W_{jo}}$. $\mathbf{Y_{jo}}$ and $\mathbf{W_{jo}}$ are the vectors composed of the odd elements of **Y** and **W** at j th time slot respectively. To mitigate the effects of the channel, a minimum mean square error or zero-forcing can be operated on $\mathbf{Y_o}=[Y_{n,o}, Y_{n+1,o}, Y_{N+2,o}, Y_{n+3,o}]$ to obtain an estimate for $\bar{\mathbf{S}}$ as follows:

$$\hat{\bar{\mathbf{S}}} = (\mathbf{\Lambda_{ACO}^H \Lambda_{ACO}} + (a/SNR)I_{2N})^{-1}\mathbf{\Lambda_{ACO}^H Y_o} \quad (2.13)$$

where a=1 for MMSE and a=0 for ZF receivers. Due to the Hermitian symmetry condition, the symbols of **S** are repeated in $\bar{\mathbf{S}}$, hence we can add them after conjugation of the second half as follow

$$\hat{\mathbf{S}} = [\hat{\bar{S}}]_{k=0}^{N-1} + [\hat{\bar{S}}^*(2N-1-k)]_{k=0}^{N-1} \quad (2.14)$$

Finally, we use an N-point IFFT to transform $\hat{\mathbf{S}}$ back into time domain to yield $\hat{\mathbf{s}}$. Hard limiter is then made on the symbol of $\hat{\mathbf{s}}$.

CHAPTER 3

REPETITION AND CLIPPING OPTICAL SINGLE CARRIER FREQUENCY DOMAIN EQUALIZATION (RCO-SCFDE) WITH ORTHOGONAL SPACE TIME CODE

In this chapter, a new modulation scheme is proposed for IM/DD OWC system that can improve bandwidth efficiency. For ACO-SCFDE, only half subcarriers are used to carry data and another half are set to zero. The new modulation scheme, called **Repetition and Clipping Optical SCFDE** (RCO-SCFDE), has only two subcarriers set zero. Besides the information data stream will be emitted twice, which can achieve coding diversity and hence decreases Bit-Error Rate (BER). The transmitted signal block consists of the original data and a DC shift of that one. Similarly, RCO-SCFDE will be used with OSTC to enhance the performance and compared with ACO-SCFDE in terms of PAPR, complexity and BER performance in Chapter 5.

3.1 Review of Repetition and Clipping Optical Single Carrier Frequency Domain Equalization (RCO-SCFDE)

The block diagram of RCO-SCFDE is shown in Figure 3.1(a). The input complex data vector $\mathbf{s} = [s_0, s_1, \dots\dots s_{N-1}]$ drawn from 4-QAM constellation is transformed into frequency domain to yield, $\mathbf{S} = [S_0, S_1, \dots\dots S_{N-1}]$. In order to obtain Hermitian constraint, vector $\mathbf{S}$ is mapped to (2N+2)×1 frequency domain vector $\mathbf{V} = [0, S_0, S_1, \dots\dots, S_{N-1}, 0, S_{N-1}^*, S_{N-2}^*, \dots\dots, S_0^*]$. Then the vector $\mathbf{V}$ is applied to a (2N+2)-point IFFT to transform it back to the time domain vector

$\mathbf{v} = [v_0, v_1, \ldots\ldots\ v_{2N+1}]$. To make the transmitted signal positive, the vector is repeated and clipped to yield, the (4N+4)*1 vector $[\mathbf{v_+;\ v_-}]$ as follows:

$v_{+,n} =$ v_n, if $v_n>0$ $\qquad$ $v_{-,n} =$ 0, if $v_n>=0$

or = 0, if $v_n<=0$ $\qquad$ or = $-v_n$, if $v_n<0$ (3.1)

Next a CP of length L is added to $\mathbf{v_+}$ and $\mathbf{v_-}$ to yield $\tilde{\mathbf{v}}_+$ and $\tilde{\mathbf{v}}_-$, respectively. The transmitted block is denoted by the (4N+4+2L)*1 vector, $\mathbf{t} = [\tilde{\mathbf{v}}_+;\ \tilde{\mathbf{v}}_-]$.

At the receiver, CP is removed and linear convolution turns into a circular one. The received blocks are given by the (2N+2)*1 blocks **y+** and y- shown below

$$\mathbf{y_+} = \mathbf{v_+} \odot \mathbf{h} + \mathbf{w_+}$$
$$\mathbf{y_-} = \mathbf{v_-} \odot \mathbf{h} + \mathbf{w_-} \quad (3.2)$$

(2N+2)-point FFT transforms $\mathbf{y_+}$ and $\mathbf{y_-}$ to frequency domain to yield

$$\mathbf{Y_+} = \mathbf{\Lambda V_+} + \mathbf{W_+}$$
$$\mathbf{Y_-} = \mathbf{\Lambda V_-} + \mathbf{W_-} \quad (3.3)$$

MMSE or ZF equalizer applied to $\mathbf{Y_+}$ and $\mathbf{Y_-}$ yield

$$\widehat{\mathbf{V}}_+ = (\mathbf{\Lambda^H \Lambda} + (1/\mathrm{SNR})\ \mathbf{I_{2N+2}})^{-1} \mathbf{\Lambda^H Y_+}$$
$$\widehat{\mathbf{V}}_- = (\mathbf{\Lambda^H \Lambda} + (1/\mathrm{SNR})\ \mathbf{I_{2N+2}})^{-1} \mathbf{\Lambda^H Y_-} \quad (3.4)$$

The estimated vector is obtained as, $\widehat{\mathbf{V}} = \widehat{\mathbf{V}}_{+} - \widehat{\mathbf{V}}_{-}$. The transmitted symbols $\mathbf{S}$ are estimated as, $\widehat{\mathbf{S}} = [\widehat{\mathrm{V}}(\mathrm{k})]_{\mathrm{k}=1}^{\mathrm{N}} + [\widehat{\mathrm{V}}^{*}(2\mathrm{N}+2-\mathrm{k})]_{\mathrm{k}=1}^{\mathrm{N}}$ and we obtain the time domain signal by taking an N-point IFFT of $\hat{\mathrm{S}}$ followed by a hard limiter.

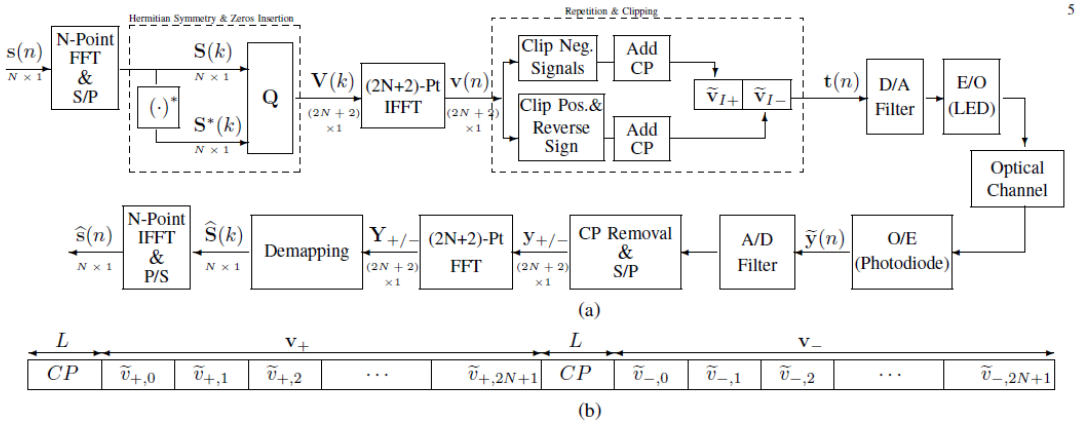

Figure 3.1 (a) RCO-SCFDE Transmitter and Receiver configuration.
(b) RCO-SCFDE symbol after cyclic extension. [10]

3.2 RCO-SCFDE with OSTC

In this section, we apply OSTC to IM/DD optical wireless using RCO-SCFDE. There are four LEDs employed in the transmitter and one photodiode in the receiver. Here we still use the same form of modified OSTC matrix, which is used in ACO-SCFDE. The modified OSTC for optical wireless transmission can be presented in this form:

$$\mathbf{V}_{4*4} = \begin{bmatrix} \mathrm{v}_1 & \mathrm{v}_2 & \mathrm{v}_3 & \mathrm{v}_4 \\ \overline{\mathrm{v}}_2 & \mathrm{v}_1 & \overline{\mathrm{v}}_4 & \mathrm{v}_3 \\ \overline{\mathrm{v}}_3 & \mathrm{v}_4 & \mathrm{v}_1 & \overline{\mathrm{v}}_2 \\ \overline{\mathrm{v}}_4 & \overline{\mathrm{v}}_3 & \mathrm{v}_2 & \mathrm{v}_1 \end{bmatrix} \tag{3.5}$$

Using this code, the blocks of symbols v_1, v_2 v_3 and v_4 modulate the LED at consecutive sample time n, n+1, n+2 and n+3 as shown in Table 2 bellow, where

$\bar{v}_i = A_i - v_i$ and A_i is the peak amplitude of the vector v_i (i=1, 2, 3, 4).

Table 3.1 RCO-SCFDE Space-Time Coding

	LED1	LED2	LED3	LED4
Time n	v_1	v_2	v_3	v_4
Time n+1	$\bar{v}_2$	v_1	$\bar{v}_4$	v_3
Time n+2	$\bar{v}_3$	v_4	v_1	$\bar{v}_2$
Time n+3	$\bar{v}_4$	$\bar{v}_3$	v_2	v_1

For RCO-SCFDE, four blocks of N complex data symbols are transmitted simultaneously. Each of LEDs is transmitting one of these blocked as in the single case described earlier (Figure 3.1).This is repeated at times n, n+1, n+2 and n+3. After passing through the channel h_1, h_2, h_3 and h_4, respectively, the received signal at these times are given by,

$$\begin{aligned} y_n &= v_1 * h_1 + v_2 * h_2 + v_3 * h_3 + v_4 * h_4 + w_n \\ y_{n+1} &= \bar{v}_2 * h_1 + v_1 * h_2 + \bar{v}_4 * h_3 + v_3 * h_4 + w_{n+1} \\ y_{n+2} &= \bar{v}_3 * h_1 + v_4 * h_2 + v_1 * h_3 + \bar{v}_2 * h_4 + w_{n+2} \\ y_{n+3} &= \bar{v}_4 * h_1 + \bar{v}_3 * h_2 + v_2 * h_3 + v_1 * h_4 + w_{n+3} \end{aligned} \quad (3.6)$$

where w_n, w_{n+1}, w_{n+2}, w_{n+3} are the additive white Gaussian noise at time n, n+1, n+2 and n+3, respectively. Removing the CP, an FFT block is applied to transform symbols of each sub-block of y_n, y_{n+1}, y_{n+2} and y_{n+3} to frequency domain to have;

$$Y_{+,n} = \boldsymbol{\Lambda_1 V_{1+}} + \boldsymbol{\Lambda_2 V_{2+}} + \boldsymbol{\Lambda_3 V_{3+}} + \boldsymbol{\Lambda_4 V_{4+}} + W_n$$

$$Y_{+,n+1} = \boldsymbol{\Lambda_1 \overline{V}_{2+}} + \boldsymbol{\Lambda_2 V_{1+}} + \boldsymbol{\Lambda_3 \overline{V}_{4+}} + \boldsymbol{\Lambda_4 V_{3+}} + W_{n+1}$$

$$Y_{+,n+2} = \boldsymbol{\Lambda_1 \overline{V}_{3+}} + \boldsymbol{\Lambda_2 V_{4+}} + \boldsymbol{\Lambda_3 V_{1+}} + \boldsymbol{\Lambda_4 \overline{V}_{2+}} + W_{n+2}$$

$$Y_{+,n+3} = \boldsymbol{\Lambda_1 \overline{V}_{4+}} + \boldsymbol{\Lambda_2 \overline{V}_{3+}} + \boldsymbol{\Lambda_3 V_{2+}} + \boldsymbol{\Lambda_4 V_{1+}} + W_{n+3} \quad (3.7)$$

where $Y_{+,n}$, $Y_{+,n+1}$, $Y_{+,n+2}$, $Y_{+,n+3}$ are the FFT of y_n, y_{n+1}, y_{n+2}, y_{n+3}, respectively. Eq. (3.7) can be rewritten in matrix form as:

$$\begin{bmatrix} Y_{+,n} \\ \overline{Y}_{+,n+1} \\ \overline{Y}_{+,n+2} \\ \overline{Y}_{+,n+3} \end{bmatrix} = \begin{bmatrix} \boldsymbol{\Lambda_1} & \boldsymbol{\Lambda_2} & \boldsymbol{\Lambda_3} & \boldsymbol{\Lambda_4} \\ \boldsymbol{\Lambda_2} & -\boldsymbol{\Lambda_1} & \boldsymbol{\Lambda_4} & -\boldsymbol{\Lambda_3} \\ \boldsymbol{\Lambda_3} & -\boldsymbol{\Lambda_4} & -\boldsymbol{\Lambda_1} & \boldsymbol{\Lambda_2} \\ \boldsymbol{\Lambda_4} & \boldsymbol{\Lambda_3} & -\boldsymbol{\Lambda_2} & -\boldsymbol{\Lambda_1} \end{bmatrix} \begin{bmatrix} \boldsymbol{V_{1+}} \\ \boldsymbol{V_{2+}} \\ \boldsymbol{V_{3+}} \\ \boldsymbol{V_{4+}} \end{bmatrix} + \begin{bmatrix} W_n \\ W_{n+1} \\ W_{n+2} \\ W_{n+3} \end{bmatrix} \quad (3.8)$$

where $\overline{Y}_{n+1} = Y_{n+1} - A_2\Lambda_1 - A_4\Lambda_3$, $\overline{Y}_{n+2} = Y_{n+2} - A_3\Lambda_1 - A_2\Lambda_4$, $\overline{Y}_{n+3} = Y_{n+3} - A_4\Lambda_1 - A_3\Lambda_2$. Λ_i (i=1, 2, 3 and 4) is the frequency response of the channel between the i th LED and the photodiode. In vector notation (3.8) can be rewritten as:

$$\boldsymbol{Z_{RCO}} \triangleq \boldsymbol{\Lambda_{RCO} V_{RCO}} + \boldsymbol{W_{RCO}} \quad (3.9)$$

Four blocks of the transmitted symbols: $\boldsymbol{V_{1+}}$, $\boldsymbol{V_{2+}}$, V_{3+} and V_{4+} are detected, using MMSE equalizer to yield:

$$\boldsymbol{\widehat{V}_+} = (\boldsymbol{\Lambda_{RCO}}^{\boldsymbol{H}} \boldsymbol{\Lambda_{RCO}} + (1/\mathrm{SNR})\mathbf{I_N})^{-\mathbf{1}} \boldsymbol{\Lambda_{RCO}}^{\boldsymbol{H}} \boldsymbol{Y_+} \quad (3.10)$$

$\mathbf{V}_{-}$, are obtained similarly. The frequency domain symbols X are estimated as

$$\widehat{\mathbf{V}} = \widehat{\mathbf{V}}_{+} - \widehat{\mathbf{V}}_{-} \tag{3.11}$$

An IFFT is used to transform $\widehat{\mathbf{V}}$, which is formed by $\mathbf{V_1}$, $\mathbf{V_2}$, $\mathbf{V_3}$ and $\mathbf{V_4}$ to time domain to obtain $\hat{\mathbf{v}}_{\mathbf{1}}$, $\hat{\mathbf{v}}_{\mathbf{2}}$, $\hat{\mathbf{v}}_{\mathbf{3}}$ and $\hat{\mathbf{v}}_{\mathbf{4}}$ in the detected blocks.

CHAPTER 4

DECOMPOSED QUADRATURE OPTICAL SINGLE CARRIER FREQUENCY DOMAIN EQUALIZATION (DQO-SCFDE) WITH ORTHOGONAL SPACE TIME CODE

In this chapter, a new technique is used to generate the real positive symbols for IM/DD OWC system. This new modulation scheme is called Decomposed Quadrature Optical Single Carrier Frequency Domain Equalization (DQO-SCFDE). In the previous schemes, in order to obtain real positive symbols, the electrical symbols have to be generated to fulfill Hermitian symmetry constraint. After that, an IFFT is applied to transform the signal into the time domain before transmission. For DQO-SCFDE, no FFT or IFFT block is used in the transmitter that can decrease the PAPR of the transmitted signal. In the DQO-SCFDE, the real and imaginary parts of complex symbols are transmitted separately. OSTC also is applied to DQO-SCFDE to enhance the performance and the results will be compared with ACO-SCFDE and RCO-SCFDE in terms of PAPR, complexity and BER performance in Chapter 5.

4.1 Review of Decomposed Quadrature Optical Single Carrier Frequency Domain Equalization (DQO-SCFDE)

The block diagram of DQO-SCFDE is shown in Figure 4.1(a). In this scheme, the real and imaginary parts of complex data symbols are transmitted separately. Let the input N complex data symbols be denoted by the block, $\mathbf{s} = [s_0, s_1, \dots \dots s_{N-1}]$,with $\mathbf{s_I} = [\mathrm{Re}(s_0), \mathrm{Re}(s_1), \dots \dots, \mathrm{Re}(s_{N-1})]and\mathbf{s_Q} = [\mathrm{Im}(s_0), \mathrm{Im}(s_1), \dots \dots, \mathrm{Re}(s_{N-1})]$ are the

vectors of real and imaginary part of **s** respectively. Then,$\mathbf{s_{I+}}, \mathbf{s_{I-}}, \mathbf{s_{Q+}}, \mathbf{s_{Q-}}$ are formed as follows:

$s_{I+}(n) = s_I(n)$, if $s_I(n)>0$ $\quad$ $s_{I-}(n) = 0$, if $s_I(n)>=0$

or = 0, if $s_I(n)<=0$ $\quad$ or = $-s_I(n)$, if $s_I(n)<0$

$s_{Q+}(n) = s_Q(n)$, if $s_Q(n)>0$ $\quad$ $s_{Q-}(n) = 0$, if $s_Q(n)>=0$

or = 0, if $s_Q(n)<=0$ $\quad$ or =$-s_Q(n)$, if $s_Q(n)<0$ (4.1)

A CP is added to each sub-block to yield the (N+L)×1 vector and 4(N+L) real and positive symbols block $\tilde{\mathbf{x}} = \left[\tilde{\mathbf{s}}_{\mathbf{I+}}, \tilde{\mathbf{s}}_{\mathbf{I-}}, \tilde{\mathbf{s}}_{\mathbf{Q+}}, \tilde{\mathbf{s}}_{\mathbf{Q-}}\right]$. After removing CP, the received sub blocks of length N corresponding to the transmitted real $\mathbf{s_{I+}}$ and $\mathbf{s_{I-}}$ are given by

$$\mathbf{y_{I+}} = \mathbf{s_{I+}} \odot \mathbf{h} + \mathbf{w_{I+}}$$
$$\mathbf{y_{I-}} = \mathbf{s_{I-}} \odot \mathbf{h} + \mathbf{w_{I-}} \quad (4.2)$$

While, the received sub-block of length N corresponding to the transmitted imaginary $\mathbf{s_{Q+}}$ and $\mathbf{s_{Q-}}$ are given by;

$$\mathbf{y_{Q+}} = \mathbf{s_{Q+}} \odot \mathbf{h} + \mathbf{w_{Q+}}$$
$$\mathbf{y_{Q-}} = \mathbf{s_{Q-}} \odot \mathbf{h} + \mathbf{w_{Q-}} \quad (4.3)$$

An N-point FFT is then performed for each received N symbols sub-block to

yield;

$$\mathbf{Y_{I+}} = \mathbf{\Lambda S_{I+}} + \mathbf{W_{I+}}$$

$$\mathbf{Y_{I-}} = \mathbf{\Lambda S_{I-}} + \mathbf{W_{I-}}$$

$$\mathbf{Y_{Q+}} = \mathbf{\Lambda S_{Q+}} + \mathbf{W_{Q+}}$$

$$\mathbf{Y_{Q-}} = \mathbf{\Lambda S_{Q-}} + \mathbf{W_{Q-}} \tag{4.4}$$

The MMSE or ZF equalizer yields

$$\hat{\mathbf{S}}_{\mathbf{I+}} = (\mathbf{\Lambda_{DQO}}^{\mathbf{H}}\mathbf{\Lambda_{DQO}} + (\mathrm{a/SNR})\mathbf{I_N})^{-1}\mathbf{\Lambda_{DQO}}^{\mathbf{H}}\mathbf{Y_{I+}}$$

$$\hat{\mathbf{S}}_{\mathbf{I-}} = \left(\mathbf{\Lambda_{DQO}}^{\mathbf{H}}\mathbf{\Lambda_{DQO}} + (\mathrm{a/SNR})\mathbf{I_N}\right)^{-1}\mathbf{\Lambda_{DQO}}^{\mathbf{H}}\mathbf{Y_{I-}}$$

$$\hat{\mathbf{S}}_{\mathbf{Q+}} = \left(\mathbf{\Lambda_{DQO}}^{\mathbf{H}}\mathbf{\Lambda_{DQO}} + (\mathrm{a/SNR})\mathbf{I_N}\right)^{-1}\mathbf{\Lambda_{DQO}}^{\mathbf{H}}\mathbf{Y_{Q+}}$$

$$\hat{\mathbf{S}}_{\mathbf{Q-}} = (\mathbf{\Lambda_{DQO}}^{\mathbf{H}}\mathbf{\Lambda_{DQO}} + (\mathrm{a/SNR})\mathbf{I_N})^{-1}\mathbf{\Lambda_{DQO}}^{\mathbf{H}}\mathbf{Y_{Q-}} \tag{4.5}$$

We form the estimated vector $\hat{\mathrm{S}}_{\mathrm{I}} = \hat{\mathbf{S}}_{\mathbf{I+}} - \hat{\mathbf{S}}_{\mathbf{I-}}$, $\hat{\mathbf{S}}_{\mathbf{Q}} = \hat{\mathbf{S}}_{\mathbf{Q+}} - \hat{\mathbf{S}}_{\mathbf{Q-}}$

The frequency domain transmitted symbols **S** are then estimated as

$$\hat{\mathbf{S}} = \hat{\mathbf{S}}_{\mathbf{I}} + \mathbf{j}\hat{\mathbf{S}}_{\mathbf{Q}} \tag{4.6}$$

The time domain signals are obtained by taking a N-point IFFT of $\hat{\mathbf{S}}$ followed by a hard limiter.

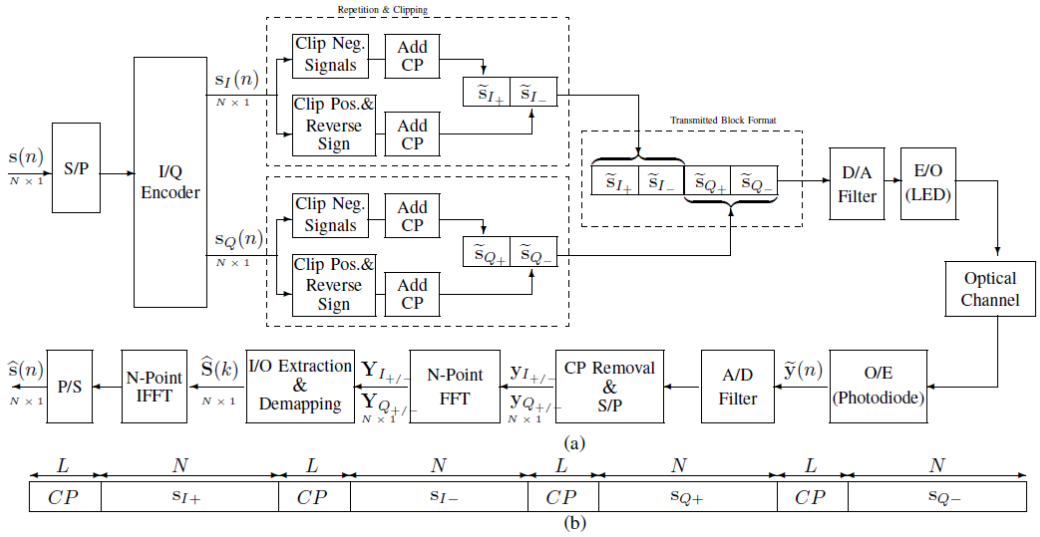

Figure 4.1 (a) DQO-SCFDE Transmitter and Receiver configuration.
(b) DQO-SCFDE symbol after cyclic extension. [10]

4.2. DQO-SCFDE with OSTC

4.2.1 OSTC DQO-SCFDE with Four LEDs and One Photodiode

Four blocks of information data symbols, drawn from constellation such as 4-QAM, 16-QAM or 64-QAM are first parsed into DQO, as follows: Let $\mathbf{s_1} = [s_{1,0}, s_{1,1}, \dots, s_{1,N-1}]$, $\mathbf{s_2} = [s_{2,0}, s_{2,1}, \dots, s_{2,N-1}]$, $\mathbf{s_3} = [s_{3,0}, s_{3,1}, \dots, s_{3,N-1}]$, $s_4 = [s_{4,0}, s_{4,1}, \dots, s_{4,N-1}]$ be the vectors of these four information streams and let $\mathbf{s_{iI}}$ and $\mathbf{s_{iQ}}$ be the vectors of the real and imaginary part of $\mathbf{s_i}$ (i=1, 2, 3, 4) respectively. Then the DQO symbols: $\mathbf{s_{1I+}}$, $\mathbf{s_{1I-}}$, $\mathbf{s_{1Q+}}$, $\mathbf{s_{1Q-}}$, $\mathbf{s_{2I+}}$, $\mathbf{s_{2I-}}$, $\mathbf{s_{2Q+}}$, $\mathbf{s_{2Q-}}$, $\mathbf{s_{3I+}}$, $\mathbf{s_{3I-}}$, $\mathbf{s_{3Q+}}$, $\mathbf{s_{3Q-}}$, $\mathbf{s_{4I+}}$, $\mathbf{s_{4I-}}$, $\mathbf{s_{4Q+}}$, $\mathbf{s_{4Q-}}$ are obtained as follows

$$s_{1I+}(n) = s_{1I}(n), \text{ if } s_{1I}(n)>0$$

$$\text{or} = \quad 0, \quad \text{if } s_{1I}(n)<=0$$

$$s_{1I-}(n) = \quad 0, \quad \text{if } s_{1I}(n)>=0$$

$$\text{or} = -s_{1I}(n), \text{ if } s_{1I}(n)>0 \tag{4.7}$$

The other DQO symbols are defined similarly. A cycle prefix (CP) is added to each sub-block to yield the symbols; $\tilde{\mathbf{s}}_{\mathbf{1I+}}$, $\tilde{\mathbf{s}}_{\mathbf{1I-}}$, $\tilde{\mathbf{s}}_{\mathbf{1Q+}}$, $\tilde{\mathbf{s}}_{\mathbf{1Q-}}$, $\tilde{\mathbf{s}}_{\mathbf{2I+}}$, $\tilde{\mathbf{s}}_{\mathbf{2I-}}$, $\tilde{\mathbf{s}}_{\mathbf{2Q+}}$, $\tilde{\mathbf{s}}_{\mathbf{2Q-}}$, $\tilde{\mathbf{s}}_{\mathbf{3I+}}$, $\tilde{\mathbf{s}}_{\mathbf{3I-}}$, $\tilde{\mathbf{s}}_{\mathbf{3Q+}}$, $\tilde{\mathbf{s}}_{\mathbf{3Q-}}$, $\tilde{\mathbf{s}}_{\mathbf{4I+}}$, $\tilde{\mathbf{s}}_{\mathbf{4I-}}$, $\tilde{\mathbf{s}}_{\mathbf{4Q+}}$, and $\tilde{\mathbf{s}}_{\mathbf{4Q-}}$. The transmitted 4(N+L) real and positive symbol blocks are given by,

$$\mathbf{x_1} = [\ \tilde{\mathbf{s}}_{\mathbf{1I+}}, \tilde{\mathbf{s}}_{\mathbf{1I-}}, \tilde{\mathbf{s}}_{\mathbf{1Q+}}, \tilde{\mathbf{s}}_{\mathbf{1Q-}}]$$

$$\mathbf{x_2} = [\ \tilde{\mathbf{s}}_{\mathbf{2I+}}, \tilde{\mathbf{s}}_{\mathbf{2I-}}, \tilde{\mathbf{s}}_{\mathbf{2Q+}}, \tilde{\mathbf{s}}_{\mathbf{2Q-}}]$$

$$\mathbf{x_3} = [\ \tilde{\mathbf{s}}_{\mathbf{3I+}}, \tilde{\mathbf{s}}_{\mathbf{3I-}}, \tilde{\mathbf{s}}_{\mathbf{3Q+}}, \tilde{\mathbf{s}}_{\mathbf{3Q-}}]$$

$$\mathbf{x_4} = [\ \tilde{\mathbf{s}}_{\mathbf{4I+}}, \tilde{\mathbf{s}}_{\mathbf{4I-}}, \tilde{\mathbf{s}}_{\mathbf{4Q+}}, \tilde{\mathbf{s}}_{\mathbf{4Q-}}] \tag{4.8}$$

Using this code, the blocks of symbols x_1, x_2 x_3 and x_4 modulate the LED consecutive sample time n, n+1, n+2 and n+3 as shown in Table 4, where $\bar{x}_i = A_i - x_i$ and A_i is the peak amplitude of the vector x_i (i=1, 2, 3, 4).

Table 4.1 DQO-SCFDE Space-Time Coding

	LED1	LED2	LED3	LED4
Time n	x_1	x_2	x_3	x_4
Time n+1	$\bar{x}_2$	x_1	$\bar{x}_4$	x_3
Time n+2	$\bar{x}_3$	x_4	x_1	$\bar{x}_2$
Time n+3	$\bar{x}_4$	$\bar{x}_3$	x_2	x_1

After passing through the channel h_1, h_2, h_3 and h_4 the received signal at time n, n+1, n+2 and n+3 are given by,

$$\begin{aligned} y_n &= \mathbf{x_1} * \mathbf{h_1} + \mathbf{x_2} * \mathbf{h_2} + \mathbf{x_3} * \mathbf{h_3} + \mathbf{x_4} * \mathbf{h_4} + w_n \\ y_{n+1} &= \bar{\mathbf{x}}_\mathbf{2} * \mathbf{h_1} + \mathbf{x_1} * \mathbf{h_2} + \bar{\mathbf{x}}_\mathbf{4} * \mathbf{h_3} + \mathbf{x_3} * \mathbf{h_4} + w_{n+1} \\ y_{n+2} &= \bar{\mathbf{x}}_\mathbf{3} * \mathbf{h_1} + \mathbf{x_4} * \mathbf{h_2} + \mathbf{x_1} * \mathbf{h_3} + \bar{\mathbf{x}}_\mathbf{2} * \mathbf{h_4} + w_{n+2} \\ y_{n+3} &= \bar{\mathbf{x}}_\mathbf{4} * \mathbf{h_1} + \bar{\mathbf{x}}_\mathbf{3} * \mathbf{h_2} + \mathbf{x_2} * \mathbf{h_3} + \mathbf{x_1} * \mathbf{h_4} + w_{n+3} \end{aligned} \quad (4.9)$$

where w_n, w_{n+1}, w_{n+2}, w_{n+3} are the additive white Gaussian noises at time n, n+1, n+2 and n+3, respectively. After removing the CP, an FFT block is applied to transform symbols of each sub-block of y_n, y_{n+1}, y_{n+2} and y_{n+3} to frequency domain,

$$\begin{aligned} \mathbf{Y_{I+,n}} &= \mathbf{\Lambda_1 X_{1I+}} + \mathbf{\Lambda_2 X_{2I+}} + \mathbf{\Lambda_3 X_{3I+}} + \mathbf{\Lambda_4 X_{4I+}} + W_{I+,n} \\ \mathbf{Y_{I+,n+1}} &= \mathbf{\Lambda_1 \bar{X}_{2I+}} + \mathbf{\Lambda_2 X_{1I+}} + \mathbf{\Lambda_3 \bar{X}_{4I+}} + \mathbf{\Lambda_4 X_{3I+}} + W_{I+,n+1} \\ \mathbf{Y_{I+,n+2}} &= \mathbf{\Lambda_1 \bar{X}_{3I+}} + \mathbf{\Lambda_2 X_{4I+}} + \mathbf{\Lambda_3 X_{1I+}} + \mathbf{\Lambda_4 \bar{X}_{2I+}} + W_{I+,n+2} \\ \mathbf{Y_{I+,n+3}} &= \mathbf{\Lambda_1 \bar{X}_{4I+}} + \mathbf{\Lambda_2 \bar{X}_{3I+}} + \mathbf{\Lambda_3 X_{2I+}} + \mathbf{\Lambda_4 X_{1I+}} + W_{I+,n+3} \end{aligned} \quad (4.10)$$

where, $\mathbf{Y_{I+,n}}$, $\mathbf{Y_{I+,n+1}}$, $\mathbf{Y_{I+,n+2}}$, $\mathbf{Y_{I+,n+3}}$ are the FFT of $\mathbf{y_n}$, $\mathbf{y_{n+1}}$, $\mathbf{y_{n+2}}$, $\mathbf{y_{n+3}}$, respectively. Eq. (4.10) can be written in matrix form as

$$\begin{bmatrix} \mathbf{Y_{I+,n}} \\ \bar{\mathbf{Y}}_\mathbf{I+,n+1} \\ \bar{\mathbf{Y}}_\mathbf{I+,n+2} \\ \bar{\mathbf{Y}}_\mathbf{I+,n+3} \end{bmatrix} = \begin{bmatrix} \mathbf{\Lambda_1} & \mathbf{\Lambda_2} & \mathbf{\Lambda_3} & \mathbf{\Lambda_4} \\ \mathbf{\Lambda_2} & -\mathbf{\Lambda_1} & \mathbf{\Lambda_4} & -\mathbf{\Lambda_3} \\ \mathbf{\Lambda_3} & -\mathbf{\Lambda_4} & -\mathbf{\Lambda_1} & \mathbf{\Lambda_2} \\ \mathbf{\Lambda_4} & \mathbf{\Lambda_3} & -\mathbf{\Lambda_2} & -\mathbf{\Lambda_1} \end{bmatrix} \begin{bmatrix} \mathbf{X_{1I+}} \\ \mathbf{X_{2I+}} \\ \mathbf{X_{3I+}} \\ \mathbf{X_{4I+}} \end{bmatrix} + \begin{bmatrix} W_{I+,n} \\ W_{I+,n+1} \\ W_{I+,n+2} \\ W_{I+,n+3} \end{bmatrix} \quad (4.11)$$

where $\bar{\mathbf{Y}}_{\mathbf{I+,n+1}} = \mathbf{Y}_{\mathbf{I+,n+1}} - \mathbf{A_2\Lambda_1} - \mathbf{A_4\Lambda_3}$, $\bar{\mathbf{Y}}_{\mathbf{I+,n+2}} = \mathbf{Y}_{\mathbf{I+,n+2}} - \mathbf{A_3\Lambda_1} - \mathbf{A_2\Lambda_4}$, $\bar{\mathbf{Y}}_{\mathbf{I+,n+3}} = \mathbf{Y}_{\mathbf{I+,n+3}} - \mathbf{A_4\Lambda_1} - \mathbf{A_3\Lambda_2}$. $\mathbf{\Lambda_i}$ (i=1, 2, 3 and 4) is the frequency response of the channel between LED and photodiode. In vector notation Eq. (4.11) can be written as

$$\mathbf{Z}_{\mathbf{I+}} \triangleq \mathbf{\Lambda}_{\mathbf{DQO}}\mathbf{S}_{\mathbf{I+}} + \mathbf{\Omega}_{\mathbf{I+}} \tag{4.12}$$

Note that Λ_{DQO} is a 4N×4N orthogonal matrix and $\Lambda_{DQO}{}^{H}\Lambda_{DQO}$ is a diagonal matrix shown below:

$$\Lambda_{DQO}{}^{H}\Lambda_{DQO} = H_{DQO}{}^{2}.H_o =$$

$$H_{DQO}{}^{2} \cdot \begin{bmatrix} 1 & H_{O1} & H_{O2} & H_{O3} \\ -H_{O1} & 1 & -H_{O3} & H_{O2} \\ H_{O2} & H_{O3} & 1 & H_{O1} \\ -H_{O3} & H_{O2} & -H_{O1} & 1 \end{bmatrix} \tag{4.13}$$

$H_{DQO}{}^{2}$ is the overall channel diversity gain, $H_{DQO}{}^{2} = |H_1|^2 + |H_2|^2 + |H_3|^2 + |H_4|^2$.

H_o is the channel dependent interference whose parameters are given by:

$$H_{O1} = \frac{2jIm(H_1^*H_2 + H_4^*H_3)}{H_{DQO}{}^{2}}$$

$$H_{O2} = \frac{2jIm(H_1^*H_3 + H_2^*H_4)}{H_{DQO}{}^{2}}$$

$$H_{O3} = \frac{2jIm(H_1^*H_4 + H_3^*H_2)}{H_{DQO}{}^{2}} \tag{4.14}$$

Four blocks of the transmitted symbols; $\mathbf{X_{1I+}}$, $\mathbf{X_{2I+}}$, $\mathbf{X_{3I+}}$**and** $\mathbf{X_{4I+}}$ are detected.

The MMSE equalizer yields

$$\mathbf{X_{I+}} = (\mathbf{\Lambda_{DQO}}^{\mathbf{H}}\mathbf{\Lambda_{DQO}} + (1/\mathrm{SNR})\mathbf{I_N})^{-1}\mathbf{\Lambda_{DQO}}^{\mathbf{H}}\mathbf{Y_{I+}} \tag{4.15}$$

$\mathbf{X_{I-}}$, $\mathbf{X_{Q+}}$, $\mathbf{X_{Q-}}$ can be obtained similarly. Note that

$$\mathbf{X_I} = \mathbf{X_{I+}} - \mathbf{X_{I-}}$$
$$\mathbf{X_Q} = \mathbf{X_{Q+}} - \mathbf{X_{Q-}} \tag{4.16}$$

The frequency domain symbols X are estimated as

$$\mathbf{X} = \mathbf{X_I} + \mathbf{jX_Q} \tag{4.17}$$

An IFFT can be used to transform X, which is formed by $\mathbf{X_1}$, $\mathbf{X_2}$, $\mathbf{X_3}$ **and** $\mathbf{X_4}$ to time domain and then $\hat{\mathbf{x}}_\mathbf{1}$, $\hat{\mathbf{x}}_\mathbf{2}$, $\hat{\mathbf{x}}_\mathbf{3}$ **and** $\hat{\mathbf{x}}_\mathbf{4}$ are detected.

4.2.2 OSTC DQO-SCFDE with Four LEDs and Two Photodiodes

We consider that multiple receiver antennas can be used to SCFDE with space-time coding when higher diversity gain is required. Before transmitted, the operation of four blocks of information data symbols is identical to the case of a single photodiode. The channels between four LEDs and two photodiodes are shown in Table 4.2 and the received signals at time n, n+1, n+2 and n+3 are shown in Table 4.3.

Table 4.2 Channels between LED and Photodiode

	Photodiode 1	Photodiode 2
LED 1	h_{11}	h_{12}
LED 2	h_{21}	h_{22}
LED 3	h_{31}	h_{32}
LED 4	h_{41}	h_{42}

Table 4.3 Received signals at time n, n+1, n+2 and n+3

	Photodiode 1	Photodiode 2
Time n	$y_{1,n}$	$y_{2,n}$
Time n+1	$y_{1,n+1}$	$y_{2,n+1}$
Time n+2	$y_{1,n+2}$	$y_{2,n+2}$
Time n+3	$y_{1,n+3}$	$y_{2,n+3}$

The transmit signals at time n, n+1, n+2 and n+3 are identical to the former case shown in Table 4.1. The received signals at photodiode 1 are given by:

$$
\begin{aligned}
y_{1,n} &= \mathbf{x_1} * \mathbf{h_{11}} + \mathbf{x_2} * \mathbf{h_{21}} + \mathbf{x_3} * \mathbf{h_{31}} + \mathbf{x_4} * \mathbf{h_{41}} + w_{1,n} \\
y_{1,n+1} &= \bar{\mathbf{x}}_{\mathbf{2}} * \mathbf{h_{11}} + \mathbf{x_1} * \mathbf{h_{21}} + \bar{\mathbf{x}}_{\mathbf{4}} * \mathbf{h_{31}} + \mathbf{x_3} * \mathbf{h_{41}} + w_{1,n+1} \\
y_{1,n+2} &= \bar{\mathbf{x}}_{\mathbf{3}} * \mathbf{h_{11}} + \mathbf{x_4} * \mathbf{h_{21}} + \mathbf{x_1} * \mathbf{h_{31}} + \bar{\mathbf{x}}_{\mathbf{2}} * \mathbf{h_{41}} + w_{1,n+2} \\
y_{1,n+3} &= \bar{\mathbf{x}}_{\mathbf{4}} * \mathbf{h_{11}} + \bar{\mathbf{x}}_{\mathbf{3}} * \mathbf{h_{21}} + \mathbf{x_2} * \mathbf{h_{31}} + \mathbf{x_1} * \mathbf{h_{41}} + w_{1,n+3}
\end{aligned} \tag{4.18}
$$

The received signals at photodiode 2 are given by:

$$
\begin{aligned}
y_{2,n} &= \mathbf{x_1} * \mathbf{h_{12}} + \mathbf{x_2} * \mathbf{h_{22}} + \mathbf{x_3} * \mathbf{h_{32}} + \mathbf{x_4} * \mathbf{h_{42}} + w_{2,n} \\
y_{2,n+1} &= \bar{\mathbf{x}}_\mathbf{2} * \mathbf{h_{12}} + \mathbf{x_1} * \mathbf{h_{22}} + \bar{\mathbf{x}}_\mathbf{4} * \mathbf{h_{32}} + \mathbf{x_3} * \mathbf{h_{42}} + w_{2,n+1} \\
y_{2,n+2} &= \bar{\mathbf{x}}_\mathbf{3} * \mathbf{h_{12}} + \mathbf{x_4} * \mathbf{h_{22}} + \mathbf{x_1} * \mathbf{h_{32}} + \bar{\mathbf{x}}_\mathbf{2} * \mathbf{h_{42}} + w_{2,n+2} \\
y_{2,n+3} &= \bar{\mathbf{x}}_\mathbf{4} * \mathbf{h_{12}} + \bar{\mathbf{x}}_\mathbf{3} * \mathbf{h_{22}} + \mathbf{x_2} * \mathbf{h_{32}} + \mathbf{x_1} * \mathbf{h_{42}} + w_{2,n+3}
\end{aligned} \tag{4.19}
$$

$y_{i,j}$ represents that the signal is received by the i th photodiode at time j. $w_{i,j}$ is the additive white Gaussian noise. At time n, n+1, n+2 and n+3, we combine the two received signals as follow:

$$
\begin{aligned}
y_n &= \mathbf{x_1} * (\mathbf{h_{11}} + \mathbf{h_{12}}) + \mathbf{x_2} * (\mathbf{h_{21}} + \mathbf{h_{22}}) + \mathbf{x_3} * (\mathbf{h_{31}} + \mathbf{h_{32}}) + \mathbf{x_4} * (\mathbf{h_{41}} + \mathbf{h_{42}}) + \\
& w_{1,n} + w_{2,n} \\
y_{n+1} &= \bar{\mathbf{x}}_\mathbf{2} * (\mathbf{h_{11}} + \mathbf{h_{12}}) + \mathbf{x_1} * (\mathbf{h_{21}} + \mathbf{h_{22}}) + \bar{\mathbf{x}}_\mathbf{4} * (\mathbf{h_{31}} + \mathbf{h_{32}}) + \mathbf{x_3} * (\mathbf{h_{41}} + \mathbf{h_{42}}) + \\
& w_{1,n+1} + w_{2,n+1} \\
y_{n+2} &= \bar{\mathbf{x}}_\mathbf{3} * (\mathbf{h_{11}} + \mathbf{h_{12}}) + \mathbf{x_4} * (\mathbf{h_{21}} + \mathbf{h_{22}}) + \mathbf{x_1} * (\mathbf{h_{31}} + \mathbf{h_{32}}) + \bar{\mathbf{x}}_\mathbf{2} * (\mathbf{h_{41}} + \mathbf{h_{42}}) + \\
& w_{1,n+2} + w_{2,n+2} \\
y_{n+3} &= \bar{\mathbf{x}}_\mathbf{4} * (\mathbf{h_{11}} + \mathbf{h_{12}}) + \bar{\mathbf{x}}_\mathbf{3} * (\mathbf{h_{21}} + \mathbf{h_{22}}) + \mathbf{x_2} * (\mathbf{h_{31}} + \mathbf{h_{32}}) + \mathbf{x_1} * (\mathbf{h_{41}} + \mathbf{h_{42}}) + \\
& w_{1,n+3} + w_{2,n+3}
\end{aligned} \tag{4.20}
$$

An FFT block is applied to transform symbols of each sub block of y_n, y_{n+1}, y_{n+2} and y_{n+3} to frequency domain. We can write

$$\mathbf{Y_{I+,n}} = \widehat{\mathbf{\Lambda}}_\mathbf{1}\mathbf{X_{1I+}} + \widehat{\mathbf{\Lambda}}_\mathbf{2}\mathbf{X_{2I+}} + \widehat{\mathbf{\Lambda}}_\mathbf{3}\mathbf{X_{3I+}} + \widehat{\mathbf{\Lambda}}_\mathbf{4}\mathbf{X_{4I+}} + \mathrm{W_{I+,n}}$$

$$\mathbf{Y_{I+,n+1}} = \widehat{\mathbf{\Lambda}}_\mathbf{1}\overline{\mathbf{X}}_\mathbf{2I+} + \widehat{\mathbf{\Lambda}}_\mathbf{2}\mathbf{X_{1I+}} + \widehat{\mathbf{\Lambda}}_\mathbf{3}\overline{\mathbf{X}}_\mathbf{4I+} + \widehat{\mathbf{\Lambda}}_\mathbf{4}\mathbf{X_{3I+}} + \mathrm{W_{I+,n+1}}$$

$$\mathbf{Y_{I+,n+2}} = \widehat{\mathbf{\Lambda}}_\mathbf{1}\overline{\mathbf{X}}_\mathbf{3I+} + \widehat{\mathbf{\Lambda}}_\mathbf{2}\mathbf{X_{4I+}} + \widehat{\mathbf{\Lambda}}_\mathbf{3}\mathbf{X_{1I+}} + \widehat{\mathbf{\Lambda}}_\mathbf{4}\overline{\mathbf{X}}_\mathbf{2I+} + \mathrm{W_{I+,n+2}}$$

$$\mathbf{Y_{I+,n+3}} = \widehat{\mathbf{\Lambda}}_\mathbf{1}\overline{\mathbf{X}}_\mathbf{4I+} + \widehat{\mathbf{\Lambda}}_\mathbf{2}\overline{\mathbf{X}}_\mathbf{3I+} + \widehat{\mathbf{\Lambda}}_\mathbf{3}\mathbf{X_{2I+}} + \widehat{\mathbf{\Lambda}}_\mathbf{4}\mathbf{X_{1I+}} + \mathrm{W_{I+,n+3}} \qquad (4.21)$$

$$\mathrm{W_{I+,n}} = \mathrm{W_{1I+,n}} + \mathrm{W_{2I+,n}}$$

$$\mathrm{W_{I+,n+1}} = \mathrm{W_{1I+,n+1}} + \mathrm{W_{2I+,n+1}}$$

$$\mathrm{W_{I+,n+2}} = \mathrm{W_{1I+,n+2}} + \mathrm{W_{2I+,n+2}}$$

$$\mathrm{W_{I+,n+3}} = \mathrm{W_{1I+,n+3}} + \mathrm{W_{2I+,n+3}} \qquad (4.22)$$

where, as before $\mathbf{Y_{I+,n}}, \mathbf{Y_{I+,n+1}}, \mathbf{Y_{I+,n+2}}, \mathbf{Y_{I+,n+3}}$ are the FFT of $\mathbf{y_n}, \mathbf{y_{n+1}}, \mathbf{y_{n+2}}, \mathbf{y_{n+3}}$, respectively. Eq. (4.21) and (4.22), can be written in matrix form as

$$\begin{bmatrix} \mathbf{Y_{I+,n}} \\ \overline{\mathbf{Y}}_\mathbf{I+,n+1} \\ \overline{\mathbf{Y}}_\mathbf{I+,n+2} \\ \overline{\mathbf{Y}}_\mathbf{I+,n+3} \end{bmatrix} = \begin{bmatrix} \widehat{\mathbf{\Lambda}}_\mathbf{1} & \widehat{\mathbf{\Lambda}}_\mathbf{2} & \widehat{\mathbf{\Lambda}}_\mathbf{3} & \widehat{\mathbf{\Lambda}}_\mathbf{4} \\ \widehat{\mathbf{\Lambda}}_\mathbf{2} & -\widehat{\mathbf{\Lambda}}_\mathbf{1} & \widehat{\mathbf{\Lambda}}_\mathbf{4} & -\widehat{\mathbf{\Lambda}}_\mathbf{3} \\ \widehat{\mathbf{\Lambda}}_\mathbf{3} & -\widehat{\mathbf{\Lambda}}_\mathbf{4} & -\widehat{\mathbf{\Lambda}}_\mathbf{1} & \widehat{\mathbf{\Lambda}}_\mathbf{2} \\ \widehat{\mathbf{\Lambda}}_\mathbf{4} & \widehat{\mathbf{\Lambda}}_\mathbf{3} & -\widehat{\mathbf{\Lambda}}_\mathbf{2} & -\widehat{\mathbf{\Lambda}}_\mathbf{1} \end{bmatrix} \begin{bmatrix} \mathbf{X_{1I+}} \\ \mathbf{X_{2I+}} \\ \mathbf{X_{3I+}} \\ \mathbf{X_{4I+}} \end{bmatrix} + \begin{bmatrix} \mathrm{W_{I+,n}} \\ \mathrm{W_{I+,n+1}} \\ \mathrm{W_{I+,n+2}} \\ \mathrm{W_{I+,n+3}} \end{bmatrix} \qquad (4.23)$$

where

$$\widehat{\Lambda}_1 = \Lambda_{11} + \Lambda_{12}$$

$$\widehat{\Lambda}_2 = \Lambda_{21} + \Lambda_{22}$$

$$\widehat{\Lambda}_3 = \Lambda_{31} + \Lambda_{32}$$

$$\widehat{\Lambda}_4 = \Lambda_{41} + \Lambda_{42} \qquad (4.24)$$

and $\bar{Y}_{I+,n+1} = Y_{I+,n+1} - A_2\hat{\Lambda}_1 - A_4\hat{\Lambda}_3$, $\bar{Y}_{I+,n+2} = Y_{I+,n+2} - A_3\hat{\Lambda}_1 - A_2\hat{\Lambda}_4$ and $\bar{Y}_{I+,n+3} = Y_{I+,n+3} - A_4\hat{\Lambda}_1 - A_3\hat{\Lambda}_2$. $\hat{\Lambda}_i$ (i=1, 2, 3 and 4) is the frequency response of the channel between LED and photodiode. In matrix notation we can write Eq. (4.23) as

$$Z_{I+} \triangleq \hat{\Lambda}_{DQO} S_{I+} + \Omega_{I+} \tag{4.25}$$

The $\hat{\Lambda}_{DQO}$ is a 4N×4N orthogonal matrix with diversity gain and interference parameters, which can be obtained by following the steps used in section 3.2. Four blocks of the transmitted symbols; $\mathbf{X_{1I+}}$, $\mathbf{X_{2I+}}$, $\mathbf{X_{3I+}}$ **and** $\mathbf{X_{4I+}}$ are detected. The MMSE equalizer yields

$$\mathbf{X_{I+}} = (\hat{\mathbf{\Lambda}}_{\mathbf{DQO}}{}^{\mathbf{H}}\, \hat{\mathbf{\Lambda}}_{\mathbf{DQO}} + (1/\mathrm{SNR})\mathbf{I_N})^{-1}\, \hat{\mathbf{\Lambda}}_{\mathbf{DQO}} \mathbf{Y_{I+}} \tag{4.26}$$

$\mathbf{X_{I-}}$, $\mathbf{X_{Q+}}$, $\mathbf{X_{Q-}}$ can be obtained similarly. Then we form,

$$\mathbf{X_I} = \mathbf{X_{I+}} - \mathbf{X_{I-}}$$
$$\mathbf{X_Q} = \mathbf{X_{Q+}} - \mathbf{X_{Q-}} \tag{4.27}$$

The complex symbols X are formed by,

$$\mathbf{X} = \mathbf{X_I} + \mathbf{jX_Q} \tag{4.28}$$

An IFFT can be used to transform X, which is formed by $\mathbf{X_1}$, $\mathbf{X_2}$, $\mathbf{X_3}$ **and** $\mathbf{X_4}$ to time domain and then $\hat{\mathbf{x}}_1$, $\hat{\mathbf{x}}_2$, $\hat{\mathbf{x}}_3$ **and** $\hat{\mathbf{x}}_4$ are detected.

CHAPTER 5

RESULTS AND DISCUSSION

5.1. Complexity Analysis

This subsection shows the computational complexity among three OSTC-SCFDE schemes; OSTC-ACO-SCFDE, OSTC-RCO-SCFDE and OSTC-DQO-SCFDE. First, we assume that a block of N independent complex data symbols is taken as input at all the transceivers of these three different SCFDE schemes. In OSTC-ACO-SCFDE, the main complexity is due to the N-Point FFT, 4N-Point IFFT at transmitter and 4N-Point FFT, N-Point IFFT at receiver. Thus the complexity of **OSTC-ACO-SCFDE** is of order $\mathbf{O}[\mathbf{4}(\mathbf{2}(\mathbf{4N})\mathbf{Log_2}(\mathbf{4N}) + \mathbf{2NLog_2}(\mathbf{N})]$. For OSTC-RCO-SCFDE, there is a (2N+2)-Point IFFT at transmitter and a (2N+2)-Point FFT at receiver. Note that the (2N+2)-Point FFT is taken twice because of two received blocks; $\mathbf{y_{+}}, \mathbf{y_{-}}$. It also has additional complexity of N-Point FFT and N-point-IFFT at the transmitter and receiver respectively. So the complexity of **OSTC-RCO-SCFDE** is of order $\mathbf{O}[\mathbf{4}\big(\mathbf{3}(\mathbf{2N}+\mathbf{2})\mathbf{Log_2}(\mathbf{2N}+\mathbf{2}) + \mathbf{2NLog_2}(\mathbf{N})\big)]$. In OSTC-DQO-SCFDE, there is no computational complexity at the transmitter. An N-Point FFT is used four times to transform the received data symbol blocks; $\mathbf{y_{I+}}, \mathbf{y_{I-}}, \mathbf{y_{Q+}}$ **and** $\mathbf{y_{Q-}}$**.** Another N-Point IFFT is taken to obtain time domain data symbols. Hence the complexity of **OSTC-DQO-SCFDE** can be given as of order $\mathbf{O[4}(\mathbf{4NLog_2}(\mathbf{N}) + \mathbf{NLog_2}(\mathbf{N}))\mathbf{]}$**.** For 4×2 OSTC-DQO-SCFDE, the order of complexity is the same with OSTC-DQO-SCFDE scheme. However the received signal is the superposition of the same data stream passing through two different optical channels, the detector of the scheme with two receivers must be a little more complicated

than that with one receiver. The order of complexity of each scheme is summarized in Table 5.1 and Figure 5.1 displays them as a function of the input block size N.

Table 5.1 Comparisons of Computational Complexity of the Three Schemes

Schemes	Complexity
OSTC-ACO-SCFDE	O $4(2(4N)\mathrm{Log}_2(4N) + 2N\mathrm{Log}_2(N))$
OSTC-RCO-SCFDE	O $4(3(2N+2)\mathrm{Log}_2(2N+2) + 2N\mathrm{Log}_2(N))$
OSTC-DQO-SCFDE	O $4(4N\mathrm{Log}_2(N) + N\mathrm{Log}_2(N))$
4×2 OSTC-DQO-SCFDE	O $4(4N\mathrm{Log}_2(N) + N\mathrm{Log}_2(N))$

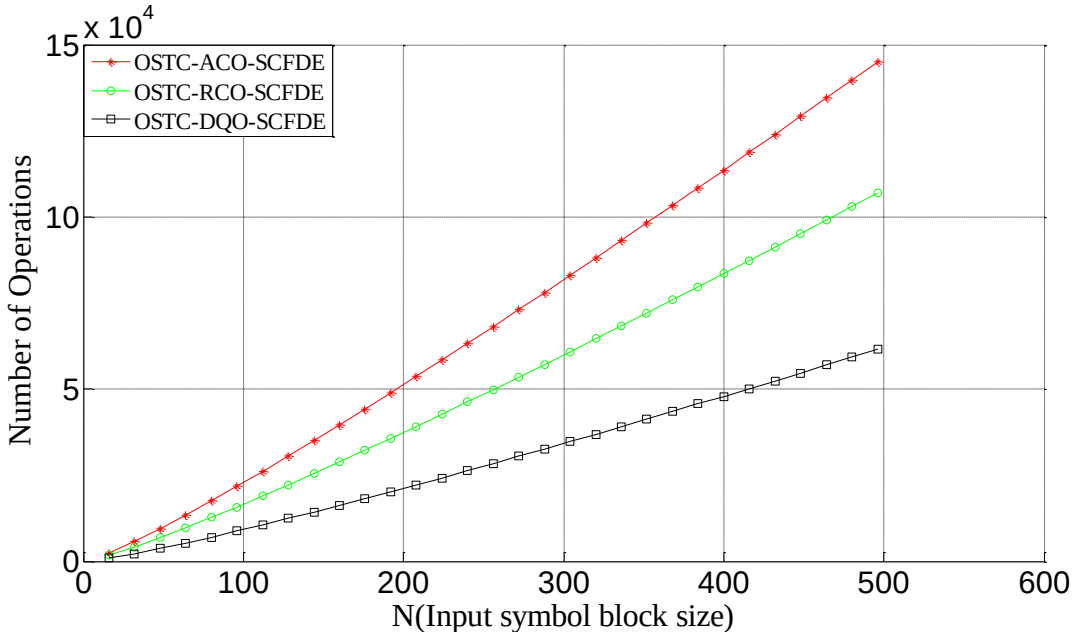

Figure 5.1 Computational Complexity Comparisons of the Three OSTC-SCFDE Schemes.

5.2. Performance Results Simulations

First, we compare the **PAPR of the three OSTC-SCFDE** schemes as shown in Figure

5.2. We notice that OSTC-DQO-SCFDE has the lowest PAPR while the other two have very similar PAPR in both cases of 4-QAM and 16-QAM. Hence DQO-SCFDE is more attractive in term of PAPR. A large PAPR signal severely affects the performance because it is not easy to obtain an LED with a linear wide dynamic power range.

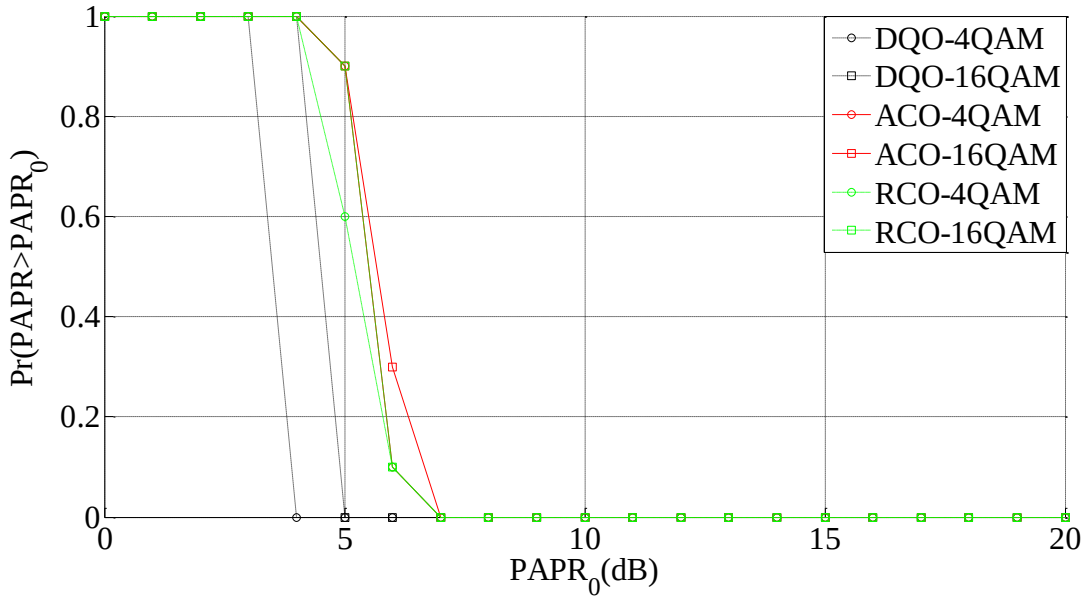

Figure 5.2 CCDF of PAPR comparisons of the three OSTC-SCFDE schemes with 4-QAM and 16-QAM.

Next the **BER performance** of single emitter SCFDE and OSTC-SCFDE is exhibited in Figure 5.3. The worst of the three BER curves of the OSTC-SCFDE OSTC is that of the ACO-SCFDE. For single emitter, DQO-SCFDE gives the best BER performance in all SNR cases. RCO-SCFDE performs similarly with DQO-SCFDE, but it is a little worse than later one. We notice that the BER performance is improved remarkably when OSTC is applied to any single emitter SCFDE scheme. All OSTC-SCFDE have about 7dB better BER performance due to the fact that it is able to

achieve channel diversity gain by using four emitters at transmitter. For OSTC-SCFDE, DQO scheme still performs better than the other two although ACO scheme gives a little bit better from 7dB to 10dB. Finally the curve with square presents BER of 4×2 OSTC-DQO-SCFDE. Because of passing through different channels, one transmitted block can obtain much more channel diversity gain by deploying two photodiodes at receiver. Obviously, 4×2 OSTC-DQO-SCFDE has a 3dB better BER performance than OSTC-DQO-SCFDE.

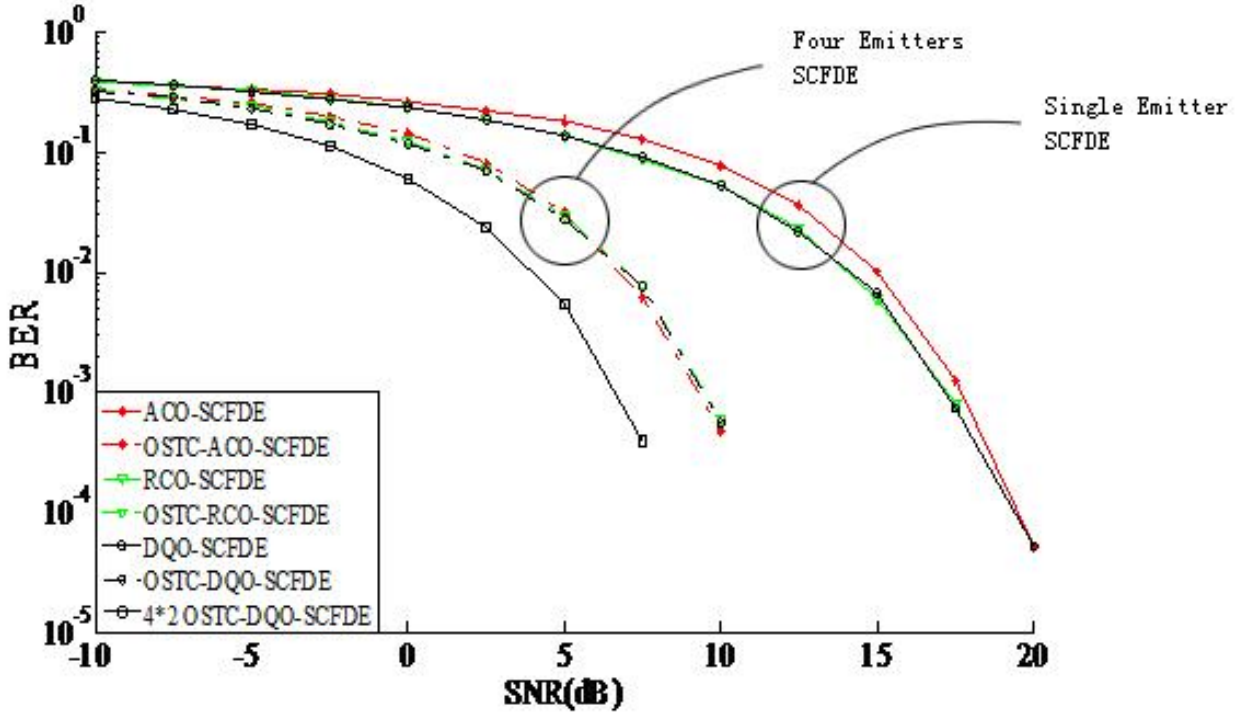

Figure 5.3 BER comparisons of Single Emitter SCFDE and OSTC-SCFDE.

CHAPTER 6

CONCLUSION AND FUTURE WORK

The objective of this thesis has been successfully achieved. Applying OSTC into optical SCFDE systems; ACO-SCFDE, RCO-SCFDE and DQO-SCFDE. The BER performances of these three are enhanced remarkably because of the channel diversity gain brought about by orthogonal coding. OSTC SCFDE can keep the same low PAPR as that of single emitter SCFDE because new schemes only require four emitters to transform four blocks of optical data symbols without any change on SCFDE. However it is obviously notable that there is a trade-off between complexity and performance. The computational complexity of OSTC SCFDEs increases intensively and is much more complicated than single emitter SCFDE. Fortunately DQO-SCFDE only requires some simple operations, such as mapping, clipping and shift. Therefore the computational complexity does not increase remarkably. Moreover the 4×2 OSTC DQO-SCFDE, which has four LEDs and two photodiodes, shows the lowest BER performance with the same order of complexity of 4×1 OSTC DQO-SCFDE. It can be confidently trusted that 4×2 OSTC DQO-SCFDE should be the most attractive choice for the use of indoor IM/DD OWC system.

During research several STCs, such as Alamouti coding and Quasi-OSTC were also investigated and applied to SCFDE. These coding techniques also have to be modified to make the transmitted signal fit the optical channel so that they can show the performance improvement as similar as the case of applying to radio frequency communications. However it should be noted that the Grammian matrix is not an

orthogonal one but has imaginary or real interference. The BER performances of SCFDE with Alamouti coding and OSTC give almost the same improvement because it is shown that there are only imaginary interferences in the Grammian matrix. For Quasi-OSTC, three code formats, which are ABBA code, EA code and PF code, are investigated. They have the same enhancement function in RF communications but perform differently in OW communications. When analyzing them, we found that the differences among them are the interferences generated by optical signals and channels. The Grammian matrix of ABBA code has real interferences hence it has the worst performance among the three. For EA code, although the interferences are real, they almost can be offset completely. Therefore it is able to perform almost the same as with PF code, which only has imaginary interferences. Although these effects of interferences generated in OW communication have not been investigated clearly, but one possible reason is that only real interferences can affect the quality of OW communications due to the fact that the transmitted optical signal is real and positive. Hence it is an interesting direction which is worth studying further. Another interesting topic is the characteristic of optical channel. There must exist a lot of differences as compared to radio channel. Optical Wireless communication is a research field full of amazing things, which attracts us to discover and explore deeper in the future.

REFERENCES

[1] J. M. Kahn and J. R. Barry, "Wireless infrared communications," Proc. IEEE, vol. 85, no. 2, pp. 265-298, Feb. 1997.

[2] Y. Sun, "Bandwidth-Efficient Wireless OFDM," IEEE J. Sel. Areas Commun., vol. 19, no. 11, pp. 2267-2278, Nov. 2001.

[3] D. Falconer, S. L. Ariyavisitakul, A. Benyamin-Seeyar, and B. Eidson, "Frequency domain equalization for single-carrier broadband wireless systems," IEEE Commun. Mag., pp. 58-66, Apr. 2002

[4] O. Ganzalez, R. Perez-Jimenez, S. Rodriguez, J. Rabadan, and A. Ayala, "OFDM over indoor wireless optical channel," IEEE Proc. Optoelectron, vol. 152, no. 4, pp. 199-204, Aug. 2005.

[5] J. Armstrong and A. Lowery, "Power efficient optical OFDM," Electronics Letters, vol. 42, pp. 370-372, Mar. 2006.

[6] I. E. Telatar, "Capacity of multi antenna Gaussian channels," European Transactions on Telecommunications, vol. 10, Issue 6, pp. 585-595, Nov. 1999

[7] S. M. Alamouti, "A simple transmitter diversity scheme for wireless Communi.," IEEE J. Sel. Areas Commun., vol. 16, pp. 1451-1458, Oct. 1998.

[8] B. Badic, M. Rupp, and H. Weinrichter, "Quasi-orthogonal space-time block codes: approaching optimality," in the 13th European Signal Processing Conference, Antalya, Turkey, Sep. 2005.

[9] V. Tarokh, H. Jafarkhani, and A. R. Calderbank, "Space-time block codes from orthogonal designs," IEEE Trans. Inform. Theory, vol. 45, pp. 1456-1467, Jul. 1999.

[10] K. Acolatse, Y. Bar-Ness, S. K. Wilson, "Novel Techniques of Single-Carrier Frequency-Domain Equalization for Optical Wireless Communications," EURASIP Journal on Advances in Signal Processing, vol. 2011, Sep. 2010.

[11] K. Acolatse, Y. Bar-Ness, S. K. Wilson, "SCFDE with space-time coding for IM/DD optical wireless communication," IEEE Wireless Communications and Networking Conference (WCNC), pp. 1694-1699, Mar. 2011.

[12] Y. Bar-Ness, N. Wu, "Space Time Coding for IM/DD Optical Wireless Communication using DQO-SCFDE," Submitted to IEEE Globecom 2011.